


# Retention of Gadolinium in Brain Parenchyma: Pathways for Speciation, Access, and Distribution. A Critical Review

Marlène Rasschaert, PhD,<sup>1\*</sup>  Roy O. Weller, MD, PhD,<sup>2</sup> Josef A. Schroeder, PhD,<sup>3</sup> Christoph Brochhausen, MD, PhD,<sup>3</sup> and Jean-Marc Idée, PharmD, MS<sup>1</sup>



## CME Information: Retention of Gadolinium in Brain Parenchyma: Pathways for Speciation, Access, and Distribution. A Critical Review.

If you wish to receive credit for this activity, please refer to the website: [www.wileyhealthlearning.com/JMRI](http://www.wileyhealthlearning.com/JMRI)

### Educational Objectives

Upon completion of this educational activity, participants will be better able to describe the access, outflow and retention of Gadolinium species in the brain parenchyma.

### Activity Disclosures

No commercial support has been accepted related to the development or publication of this activity.

### Faculty Disclosures:

**Editor-in-Chief:** Mark E. Schweitzer, MD, discloses no relevant financial relationships.

**CME Editor:** Mustafa R. Bashir, MD, discloses grants from CymaBay, Madrigal Pharmaceuticals, Metacrine, NGM and Pinnacle, institutional support from Clinical Research, ProSciento, and Siemens as principal investigator, and consultant fees from MedPace.

### Authors:

Authors Marlène Rasschaert, PhD and Jean-Marc Idée, PharmD, MS disclose employment at Guerbet and were not involved in the development of clinical content or recommendations for this CME activity. The remaining authors reported no conflicts of interest or financial relationships relevant to this article.

This activity underwent peer review in line with the standards of editorial integrity and publication ethics. Conflicts of interest have been identified and resolved in accordance with John Wiley and Sons, Inc.'s Policy on Activity Disclosure and Conflict of Interest.

### Accreditation

John Wiley and Sons, Inc. is accredited by the Accreditation Council for Continuing Medical Education to provide continuing medical education for physicians.

John Wiley and Sons, Inc. designates this journal-based CME activity for a maximum of 1.0 *AMA PRA Category 1 Credit*<sup>™</sup>. Physicians should only claim credit commensurate with the extent of their participation in the activity.

For information on applicability and acceptance of continuing medical education credit for this activity, please consult your professional licensing board.

This activity is designed to be completed within 1 hour. To successfully earn credit, participants must complete the activity during the valid credit period, which is up to two years from initial publication. Additionally, up to 3 attempts and a score of 70% or better is needed to pass the post test.

View this article online at [wileyonlinelibrary.com](http://wileyonlinelibrary.com). DOI: 10.1002/jmri.27124

Received Dec 6, 2019, Accepted for publication Feb 6, 2020.

\*Address reprint requests to: M.R., BP 57400 95943 Roissy CdG cedex, France. Email: [marlene.rasschaert@guerbet.com](mailto:marlene.rasschaert@guerbet.com)

From the <sup>1</sup>Guerbet, Research and Innovation Division, Aulnay-sous-Bois, France; <sup>2</sup>Neuropathology, Faculty of Medicine University of Southampton, Southampton General Hospital, Southampton, UK; and <sup>3</sup>Institute of Pathology, University of Regensburg, Regensburg, Germany

This is an open access article under the terms of the Creative Commons Attribution-NonCommercial-NoDerivs License, which permits use and distribution in any medium, provided the original work is properly cited, the use is non-commercial and no modifications or adaptations are made.

The unexpected appearance of  $T_1$  hyperintensities, mostly in the dentate nucleus and the globus pallidus, during non-enhanced MRI was reported in 2014. This effect is associated with prior repeated administrations of gadolinium (Gd)-based contrast agents (GBCAs) in patients with a functional blood–brain barrier (BBB). It is widely assumed that GBCAs do not cross the intact BBB, but the observation of these hypersignals raises questions regarding this assumption. This review critically discusses the mechanisms of Gd accumulation in the brain with regard to access pathways, Gd species, tissue distribution, and subcellular location. We propose the hypothesis that there is early access of Gd species to cerebrospinal fluid, followed by passive diffusion into the brain parenchyma close to the cerebral ventricles. When accessing areas rich in endogenous metals or phosphorus, the less kinetically stable GBCAs would dissociate, and Gd would bind to endogenous macromolecules, and/or precipitate within the brain tissue. It is also proposed that Gd species enter the brain parenchyma along penetrating cortical arteries in periarterial pial–glial basement membranes and leave the brain along intramural periarterial drainage (IPAD) pathways. Lastly, Gd/GBCAs may access the brain parenchyma directly from the blood through the BBB in the walls of capillaries. It is crucial to distinguish between the physiological distribution and drainage pathways for GBCAs and the possible dissociation of less thermodynamically/kinetically stable GBCAs that lead to long-term Gd deposition in the brain.

**Level of Evidence:** 5.

**Technical Efficacy Stage:** 3.

J. MAGN. RESON. IMAGING 2020;52:1293–1305.

**C**ONTRAST RESOLUTION of magnetic resonance imaging (MRI) is improved by the intravenous administration of contrast agents. Around 30% of MRI procedures are associated with such injections, especially for central nervous system (CNS) examinations, angiography, and breast imaging. In 2016, it was estimated that ~30 million procedures per year were contrast-enhanced.<sup>1</sup>

Until recently, it was admitted that gadolinium-based contrast agents (GBCAs) did not cross the functional blood–brain barrier (BBB)<sup>2</sup> and were immediately cleared from the central nervous system through venous drainage, thus allowing the diagnosis of tumors and other lesions where the BBB is no longer functional.

It has been common practice for a large number of GBCA-enhanced MR procedures to be performed for the follow-up of benign or malignant tumors (up to 59 consecutive administrations in one study,<sup>3</sup> 86 in another<sup>4</sup>).

In early 2014, a Japanese team reported gradual  $T_1$  hyperintensities in the dentate nucleus and globus pallidus on unenhanced MR images following serial administrations of GBCAs to patients with normal renal function.<sup>5</sup> However,  $T_1$  hyperintensities are not limited to these structures, since additional areas of the brain are found to be enhanced, including the anterior pituitary gland.<sup>6</sup> This was especially noticeable in patients who received a large number of administrations of GBCA.<sup>3</sup> This causal link with tissue gadolinium (Gd) retention was confirmed by an avalanche of nonclinical and clinical studies,<sup>7</sup> including in pediatric patients<sup>8,9</sup> and healthy animals.<sup>10–14</sup> So far, there is no evidence that Gd retention leads to any neurological disorders.<sup>7</sup>

GBCAs differ according to the molecular structure of their polyaminopolycarboxylic ligand (linear or macrocyclic, ionic, or nonionic/neutral) which determines their thermodynamic properties (Table 1).

It rapidly became apparent that the gradual appearance of a  $T_1$  hypersignal in specific structures of the CNS was almost exclusively associated with prior administrations of

linear GBCAs.<sup>16,17</sup> This finding, associated with the previous causal relationship of nephrogenic systemic fibrosis with linear GBCAs,<sup>18</sup> in patients with severe renal failure prompted the European Medicines Agency to suspend the marketing authorizations for intravenous linear products.<sup>19</sup> Subsequently, the US Food and Drug Administration (FDA), while maintaining the authorization for linear GBCAs, recognized that these agents resulted in more brain retention than macrocyclics.<sup>20</sup> The FDA stated that healthcare professionals should consider the Gd retention characteristics of each compound when selecting a GBCA for patients who may be at risk. The FDA also requested radiologists to minimize repeated GBCA imaging studies and urged companies to conduct postmarketing nonclinical and clinical studies.<sup>20</sup>

Using mass spectrometry, several teams reported the presence of Gd deposits in the structures in question.<sup>21,22</sup> Interestingly, the strength of the  $T_1$  hyperintensity was correlated with the number of prior administrations of GBCAs.<sup>21</sup> These data raised a number of important questions: 1) How does Gd access the (even healthy) CNS parenchyma?; 2) In which chemical form(s)?; 3) Do all molecular categories of GBCAs behave in a similar way and, if not, why not?; 4) Where precisely does Gd accumulate?; 5) What are the pathways for elimination of Gd from the brain? 6) Is this phenomenon associated with toxic effects? We will focus on the first five of these questions (1–5). So far, there is no clinical evidence of harmful consequences of intracerebral Gd deposition.<sup>7,17</sup>

## GADOLINIUM LOCATION AND SPECIATION IN BRAIN TISSUES: CHEMICAL CONSIDERATIONS

Numerous nonclinical studies performed in small (rodents) or large (sheep, pigs) mammalian species have demonstrated that single or repeated administration of linear GBCAs leads to

TABLE 1. Main Characteristics of Gadolinium-Based Contrast Agents Currently Marketed or Under Clinical Development<sup>15</sup>

International nonproprietary name	Gadopixelon	Gadoterate	Gadobutrol	Gadoteridol	Gadobenate	Gadodiamide	Gadopentetate
Trade name	NA <sup>a</sup>	Dotarem	Gadovist/Gadavist	ProHance	MultiHance	Omniscan	Magnevist
Ligand structure	Macrocylic	Macrocylic	Macrocylic	Macrocylic	Linear	Linear	Linear
Ligand charge	Nonionic	Ionic	Nonionic	Nonionic	Ionic	Nonionic	Ionic
Osmolality at 37°C (mOsm/kg) at marketed concentration	843	1350	1603	630	1970	789	1960
Relaxivity (r <sub>1</sub> /r <sub>2</sub> ) (mM <sup>-1</sup> ·s <sup>-1</sup> )	12.2/15	2.9/3.2	3.3/3.9	2.9/3.2	4/4.3	3.3/3.6	3.3/3.9
at 37°C and 1.5 T	In biological medium	3.6/4.3	5.2/6.1	4.1/5	6.3/8.7	4.3/5.2	4.1/4.6
Log K <sub>cond</sub> (pH 7.4)	15.5	19.3	14.7	17.1	18.4	14.9	17.7
Kinetic stability in acidic conditions (HCl, pH 1.2) and 37°C	20 ± 3 days	4 ± 0.5 days	18 h	4 h	ND	<5 s	<5 s

<sup>a</sup>Gadopixelon is under clinical development.

dramatically higher concentrations of “elemental” (ie, total, regardless of the species) Gd in brain parenchyma than do macrocyclic GBCAs, when measured long after the last administration (Fig. 1).<sup>11–14,23–27</sup> This is yet again suggestive of dechelation of these highly hydrophilic molecules. Interestingly, the concentration of elemental Gd measured in brain structures of rats was found to be the highest in the deep cerebellar nuclei,<sup>27</sup> which include the dentate (lateral) nuclei; this suggests a clinical relevance for these findings.

The possibility of gradual in situ dissociation of linear GBCAs in patients was soon proposed.<sup>28</sup> This phenomenon may involve the kinetic stability of GBCAs that is far higher with macrocyclic GBCAs than with linear agents.<sup>29</sup>

In rats with renal impairment repeatedly treated with gadodiamide, the presence of soluble and dissociated Gd (representing around 90% of circulating elemental Gd) in plasma was reported 6 days after the last of 20 daily injections.<sup>26</sup>

### Brain Structure Affinities for Gd and Endogenous Metals

The question arises regarding the affinity of Gd species for certain CNS structures. Patients who receive a large (>35) number of administrations of linear GBCAs, and thus a higher cumulative dose, exhibit T<sub>1</sub> hypersignals in several brain structures (posterior thalamus, substantia nigra, red nucleus, cerebellar peduncle, colliculi), in addition to dentate nucleus and globus pallidus.<sup>3</sup> It is worth emphasizing that these structures have the particular feature of being associated with a high concentration of iron.<sup>30,31</sup> Dentate nucleus and globus pallidus are particularly rich in iron, but also copper and zinc, although at a lower concentration.<sup>32–34</sup> Interestingly, the distribution of elemental Gd concentrations among the various CNS structures correlated significantly with that of Fe in rats treated with linear GBCAs,<sup>27</sup> a result consistent with the previous feature. Laser ablation-inductively coupled plasma mass spectrometry (LA-ICP MS) studies performed in samples of sheep cerebellum showed colocalization of Gd with Zn, Fe, and Cu 10 weeks following single injections of linear GBCAs (but not after macrocyclic GBCAs).<sup>14</sup> However, in another LA-ICP-MS study performed on a single human dentate nucleus, no apparent correlation between Gd and Fe, Cu or Zn could be observed.<sup>35</sup>

If one considers that the colocalization of Gd and metals is not a hazard, several hypotheses can be proposed:

1. Endogenous Fe may exchange with Gd (transmetallation). The apparent thermodynamic stability constant values of the Fe-L chelates are often higher than those of the Gd-L chelates (L for ligand) (eg, log K<sub>cond</sub> values are 23.4 and 17.7 for Fe-DTPA and Gd-DTPA, respectively).<sup>29</sup> However, to comply with this hypothesis Fe must be labile and locally present at a high concentration. Fe is mobilized by transport or storage proteins such as ferritin, transferrin, or hemoglobin,<sup>36</sup> and the labile pool of Fe is therefore low.<sup>37</sup>

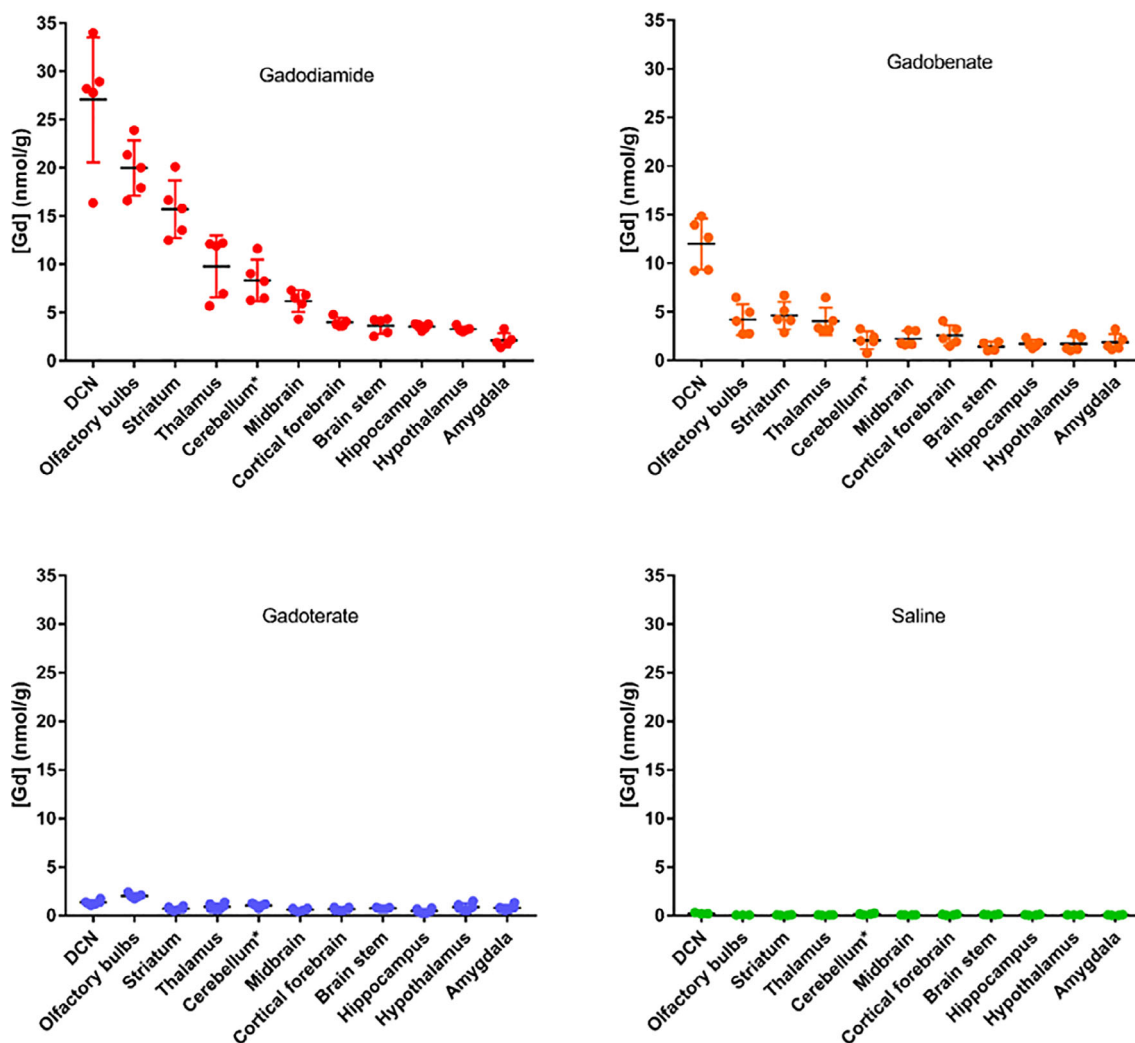
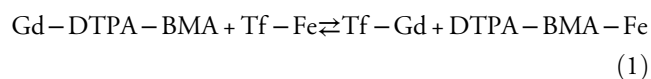


FIGURE 1: Concentrations of elemental Gd determined by inductively coupled plasma mass spectrometry in the various dissected brain areas (cerebellum\*: except for DCNs) 4½ weeks after the last injection to rats (20\*0.6 mmol Gd/kg body weight). Reprinted from Ref. 26 with permission.

The lack of reliable data on concentrations and locations of labile pools of Fe in the CNS structures of interest makes it difficult to draw conclusions on this hypothesis.

- Another hypothesis is that Gd is concentrated at the same locations as Fe because it uses the same access pathways. This would involve the prior dissociation of GBCA and the binding of Gd to Fe transporter proteins. Gd can bind transferrin (Tf) with a weaker affinity when compared to Fe.<sup>38</sup> In the case of gadodiamide (ie, Gd-DTPA-BMA), this would translate into:



The thermodynamic constant value of Fe-DTPA-BMA is greater than that of Gd-DTPA-BMA (gadodiamide) ( $\log K_{\text{therm}}$  values are 21.9 and 16.9, respectively).<sup>29</sup> However, there are two binding sites for Fe with Tf ( $\log K_{\text{cond}}$

value is 20.2 for site 1 and 39.3 for site 2).<sup>39</sup> If the respective local concentrations for the above species allow, a Gd vs. Fe transmetallation process with the first site of Tf would be possible but has not been demonstrated so far.

- GBCAs would dissociate before entering the dentate nucleus (consistent with the finding of dissociated and soluble Gd in the blood compartment<sup>26</sup>) and Gd would pass through similar pathways as endogenous metals.
- Gd from low-stability GBCAs might also exchange with ionized calcium, as previously suggested<sup>40,41</sup> (if local concentration of the latter metal allows it).

In addition to Fe, colocalization of Gd and P was reported in rat cerebellum<sup>42</sup> in addition to the postmortem human cerebellum,<sup>43,44</sup> consistent with the presence of  $\text{GdPO}_4$ . Gadolinium signal was also found by LA-ICP-MS in the dentate nucleus and cerebellar cortex of one patient who received macrocyclic GBCAs twice (the last administration was only

2 weeks before death). The Gd signal colocalized with those of Fe, Cu, Zn, and P.<sup>45</sup> Of note is that the LA-ICP-MS technique does not allow speciation studies, and therefore is by no means indicative of a putative dissociation of Gd from the macrocyclic GBCAs.

Transmission electron microscopy (TEM) studies associated with nanoscale secondary ion mass spectrometry demonstrated that P-associated Gd deposits were located in various areas of deep cerebellar nuclei (DCN).<sup>42</sup> It is worth emphasizing that TEM does not allow the study of soluble Gd species. Therefore, data from this technique should be analyzed in conjunction with other, complementary, approaches.

### Gadolinium Speciation in Brain Tissues

Gd speciation in the brain has been the subject of a large number of studies.<sup>24,25,46–49</sup> In homogenates of cerebellum from rats treated with linear agents, the presence of soluble macromolecular (250–300-kDa) Gd-containing species was observed 24 days after the last administration, while no such effect was found with macrocyclic GBCAs. Still, in linear GBCAs-treated rats, Gd was found to a large extent in the insoluble brain tissue fraction.<sup>46</sup> In a subsequent study, following repeated administrations of the linear GBCA gadodiamide to rats, insoluble species of Gd in the cerebellum were estimated to be 53% of the elemental Gd levels, while the intact Gd chelate was 18%. This suggests that an additional ~30% must have been present in the soluble fraction. It was proposed that these soluble and dissociated Gd species explained the T<sub>1</sub> hyperintensity found in the cerebellum.<sup>25</sup> One year after the last administration of a linear GBCA to rats, 75% of the elemental Gd detected in the cerebellum was bound to macromolecules (MW > 66.5 kDa) as soluble species, with the proportion increasing over time. Such an effect can be explained by the progressive binding or, alternatively, by the faster elimination of the intact linear Gd chelate.

Conversely, after repeated injection of the macrocyclic GBCA gadoterate, only traces of Gd, in the intact chelated form, were measured in the soluble fraction.<sup>24</sup> In another study, a single administration of a very high dose to mice confirmed that, after 10 days, several endogenous molecules were bound to Gd from the linear GBCA gadopentetate, while no such effect was observed with the macrocyclic GBCA gadoterate. However, Gd from the macrocyclic agent gadobutrol was also found in several molecules with molecular weight larger than GBCAs.<sup>48</sup> The reasons for this discrepancy between GBCAs are unclear. Lastly, infusion of the chelating agent Ca-DTPA 7 weeks after a single administration of a linear GBCA to rats was associated with significant excretion of Gd in the urine.<sup>47</sup> In parallel, the amount of Gd in the brain parenchyma decreased. This is consistent with mobilization of Gd from tissues. Conversely, no such effect was found after administration of a macrocyclic agent.<sup>47</sup>

Interestingly, even a single administration of a clinically-relevant dose of GBCA demonstrated that linear GBCAs resulted in significantly higher residual Gd concentrations in the cerebellar tissue than a macrocyclic GBCA at the late time-point of 5 months. Furthermore, for the linear GBCAs, two classes of Gd species were detected: intact Gd chelate and Gd bound to soluble macromolecules (>80 kDa), whereas, in the case of the macrocyclic GBCA, Gd was detected only in its chelated form.<sup>49</sup> The nature of the macromolecules that bind Gd remains unknown. Sialic acid residues or glycosaminoglycans structures on the surface of cells, or within the extracellular matrix, may be interesting targets.<sup>25,50</sup>

The most likely hypothesis is therefore that the less kinetically stable linear GBCAs gradually dissociate in tissues, while macrocyclics remain intact and are excreted unaltered in the urine (Fig. 2).

Taken together, these data are consistent with the thermodynamic characteristics of GBCAs.<sup>29,51</sup> Obviously,

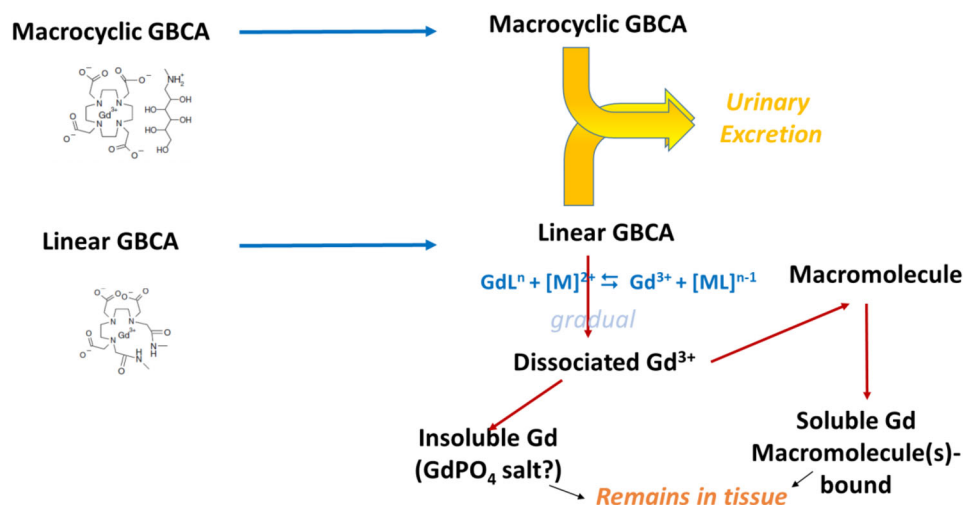
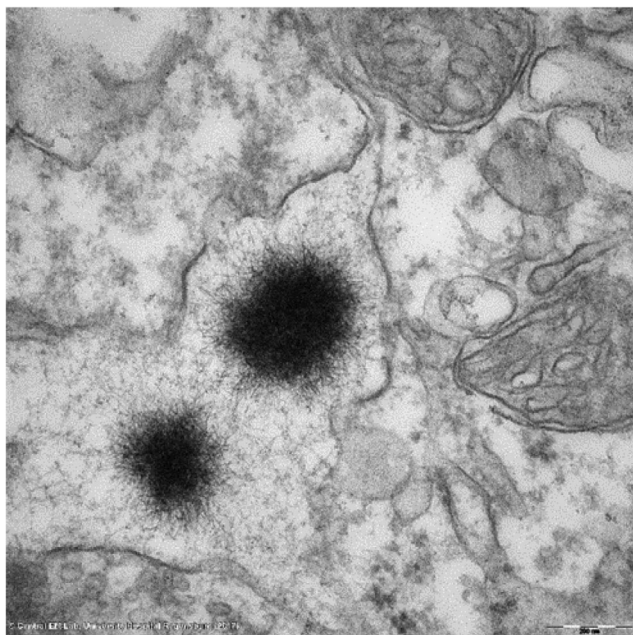


FIGURE 2: Comparative hypothetical gradual behavior of macrocyclic and linear GBCAs subsequent to their uptake by the central nervous system. GdL: chelated Gd; M: endogenous metal; ML: chelated metal.

knowledge of the nature of the macromolecule(s) that bind Gd and represent the soluble Gd species could help to make significant progress in the understanding of the distribution and retention of GBCAs in brain tissues, and possibly in the putative long-term toxicologic consequences. Future progress will probably come from combined and complementary bioanalytical techniques.

### LONG-TERM FOLLOW-UP OF GADOLINIUM CONCENTRATIONS IN THE BRAIN PARENCHYMA FOLLOWING REPEATED ADMINISTRATIONS OF GBCAS

Two teams independently followed up the concentrations of elemental Gd in the brain parenchyma of rats for up to 1 year after the last of repeated administrations of linear and macrocyclic GBCAs.<sup>24,52</sup> Both studies concurred in: 1) a lower elemental Gd concentration in the CNS at completion of the treatment period with macrocyclic GBCAs vs. linear agents; 2) with macrocyclic GBCAs, there was continuous clearance of residual Gd from the brain, with no indication of a steady-state tissue level. No such effect was observed with linear GBCAs. Furthermore, an increase in the DCN-to-brainstem T<sub>1</sub> signal intensity (SI) ratio was found with linear GBCAs and persisted for the full 1-year observation period (Fig. 3).<sup>24,52</sup> These studies clearly distinguished between normal clearance of GBCA and retention of dissociated Gd.



**FIGURE 3:** Typical "sea urchin"-shaped Gd deposit located in the interstitial space of the lateral nucleus (corresponding to the dentate nucleus in humans) of a rat repeatedly treated with gadodiamide (12 mmolGd/kg cumulated). The presence of Gd was validated by electron energy loss spectroscopy.

### CEREBRAL ANATOMICAL STRUCTURES ASSOCIATED WITH GADOLINIUM DEPOSITION

#### Organ Level

In addition to the dentate nucleus and the globus pallidus, postmortem studies demonstrated the presence of elemental Gd in the thalamus and pons of patients who received repeated administrations of gadodiamide.<sup>21</sup> Further to these structures, a gradual T<sub>1</sub> hypersignal was reported in the substantia nigra, red nucleus, cerebellar peduncle, and colliculi.<sup>3</sup> This effect is highly suggestive of Gd deposition. Interestingly, T<sub>1</sub> hypersignal was also reported in the choroid plexus (CP) of patients<sup>53</sup> and of rats.<sup>26</sup> We found a substantial concentration ( $13.2 \pm 6.4$  nmol/g) of elemental Gd in the CP dissected from rats 4 months after the last of 20 administrations of gadodiamide (36 mmolGd/kg cumulated) (unpublished data). Furthermore, 4.5 hours after a single administration of GBCAs to rats, the presence of elemental Gd was reported in the cerebrospinal fluid (CSF). Concentrations of Gd were higher in the CSF than in the blood. In this study, CSF Gd was almost completely cleared after 24 hours.<sup>54</sup> Elemental Gd was found in the CSF of adult and pediatric patients who received a single GBCA application. Higher concentrations of elemental Gd were associated with an age of at least 18 years and total proteins levels in the CSF above 35 mg/dL.<sup>55</sup> In a prior study, concentrations of elemental Gd in the CSF increased within the first 8 hours after intravenous GBCA administration, and then decreased between 8 and 48 hours. The GBCA was almost completely cleared from the CSF after 48 hours.<sup>56</sup>

Some studies demonstrated the presence of elemental Gd in other structures, especially the olfactory bulbs of mice and rats (Fig. 1).<sup>27,57,58</sup> To our knowledge, no T<sub>1</sub> signal enhancement has been reported so far in olfactory bulbs in humans or rats. Of note is that the olfactory bulb is about 0.01% of the human brain by volume and 2% of the mouse brain by volume.<sup>59</sup> Finally, it should be recalled that, in addition to the brain, numerous studies have found the sustained presence of elemental Gd in multiple organs or tissues, including the bone (cortical and bone marrow), skin, kidney, liver, etc., both in animals and patients.<sup>12,18,26,40,44,47</sup>

#### Brain Tissue Levels

Detailed localization studies, by means of LA-ICP-MS, demonstrated the presence of Gd in the granular layer of the cerebellar cortex of rats<sup>11,52</sup> and of human subjects<sup>9,35</sup> after repeated administration of linear GBCAs. Elemental Gd concentrations were similar to those measured in DCN.<sup>52</sup> No T<sub>1</sub> signal enhancement has been reported so far in cerebellar cortex, to our knowledge. This suggests that Gd is present in a mostly insoluble form at this level.



### Cellular Level

TEM studies associated with spectroscopy techniques for characterization showed the presence of electron-dense Gd deposits in the cerebellum of rats treated with linear GBCAs<sup>11,42,58,60</sup> and in patients.<sup>21,61</sup> Except for two,<sup>42,58</sup> these studies focused on the dentate nucleus or its equivalent in rats, the lateral nucleus.<sup>62</sup> Gd deposits had a spheroid and spiny shape resembling a “sea urchin,” ~200–300 nm in diameter with 2-nm-wide spines, located in the interstitial space and close to vascular basement membranes (Fig. 3). The copresence of Ca, N, and O was reported, as well as P, which is consistent with the presence of insoluble GdPO<sub>4</sub> salt in these deposits.<sup>42</sup>

Furthermore, Gd deposits were also associated with intracellular membrane-bound pigment aggregates within glial cells of the rat DCN. These pigments were identified as lipofuscin. Gd deposits were also identified in the CP of linear GBCAs-treated rats, in fibrocyte-like cells, in the interstitium located perivascularly between the basement membranes of a capillary, and also in the epithelial basement membrane of the CP.<sup>42</sup> Lastly, in specimens of human dentate nuclei, deposits of insoluble Gd were found within the nucleus of a neuron.<sup>61</sup> To our knowledge, no such finding has been reported in rats so far.

### CNS ACCESS PATHWAYS FOR GBCAS: CERTAINTIES AND ASSUMPTIONS

Intravenous route is not the only pathway for exogenous metals presenting an effect on the MRI signal. Manganese, another cation with a strong shortening effect on T<sub>1</sub> relaxation time, can easily access the blood, then the brain parenchyma through the olfactory system, as shown in welders exposed to Mn-containing fumes and who presented increased T<sub>1</sub> hyperintensity in various brain structures, especially the globus pallidus.<sup>63</sup>

Regarding, GBCAs, our hypothesis is that there are three access pathways for Gd species into the brain parenchyma, as discussed below. We propose an integrated approach for the access of GBCAs in the CNS and their normal distribution, including intraparenchymal Gd speciation.

#### Blood Cerebrospinal Fluid Barrier Access Pathway

Following systemic injection, GBCAs, regardless of their structural category (and/or possibly dissociated and soluble Gd species from less stable agents), enter the CSF compartment, as shown by direct dosage in patients who underwent lumbar puncture<sup>55</sup> or, indirectly, by T<sub>2</sub>-weighted fluid-attenuated inversion recovery (FLAIR) MRI.<sup>64–68</sup> Interestingly, this increase in the T<sub>2</sub> SI was prolonged, with a significant increase in the perineural space of the distal optic nerve sheath, perivascular spaces (PVS) of the basal ganglia, foramen magnum, and prepontine cistern, detected at 3 hours postadministration (p.a.) of a GBCA. The effect

was still noticeable 24 hours p.a.<sup>68</sup> This is consistent with data in rats where T<sub>2</sub> signal peaks in CSF-containing structures were observed at 9 or 25 minutes p.a.<sup>54</sup> The T<sub>2</sub> SI increase was also detected in the CP and brain ventricles. It is worth noting that a reduction in T<sub>2</sub> signal amplitude was in the expected direction of bulk flow of CSF, that is, from the lateral to the 3<sup>rd</sup> and 4<sup>th</sup> ventricles, then to the subarachnoid space.<sup>68</sup>

Passage of Gd species from the blood compartment to the CSF through the fenestrated and leaky<sup>69</sup> capillaries of CP, then to the CSF through the CP plexus epithelium (the “blood cerebrospinal fluid barrier” or BCSFB<sup>70</sup>), is therefore likely and consistent with the presence of insoluble Gd deposits at this level.<sup>42</sup> The exact pathway by which GBCAs cross BSCFB remains speculative. This barrier can be crossed by passive diffusion, diffusion facilitated by membrane influx (eg, solute carrier family), and efflux transporters, or through vesicular transfer or transcytosis due to the presence of non-specific mediators like vesicles-associated membrane proteins.<sup>70,71</sup> GBCAs (or other soluble Gd species) would escape efflux transporters in the CP epithelial cells, at least in part. It is likely that low-stability GBCA and/or dissociated and soluble Gd, bound to a macromolecule, are sequestered in the CP. This phenomenon would explain the T<sub>1</sub> hypersignal observed in rats<sup>26</sup> and patients with renal failure<sup>53</sup> (therefore sensitized to a higher circulating GBCA concentration). A proportion of the GBCAs would dissociate locally, as demonstrated by the presence of Gd deposits in the perivascular interstitial spaces in the CP and in the basement membranes of the CP epithelium.<sup>42</sup>

The traditional pathway for reabsorption is that, once in the CSF, soluble GBCAs are transported to the subarachnoid space to reach arachnoid granulations for eventual reabsorption into the venous blood compartment through a pressure-dependent gradient.<sup>72</sup> However, there is mounting evidence, both in humans and in rodents, that a significant proportion of CSF drains to lymph nodes, especially through the nasal mucosa via the cribriform plate of the ethmoid bone and along dural lymphatics.<sup>73–75</sup>

We propose that a fraction of soluble GBCA present in the CSF would cross the ependymal lining to access the interstitium of the brain (Fig. 4). *ex vivo* application of lanthanum nitrate to the ventricular surface of mice showed the ion winding through the extracellular spaces of the ependyma and through the interwoven extracellular spaces of the astrocyte layer.<sup>76</sup> Dissociated and soluble Gd may follow the same pathway. Following intracerebroventricular (i.c.v.) administration of the neutral agent gadodiamide to rats, the molecule was distributed from lateral ventricles to the fourth ventricle and crossed the BCSFB and the ependymal layer.<sup>77</sup> Conversely, the anionic GBCA gadopentetate injected i.c.v. to rats was confined to the intraventricular space, probably because it was repelled by the sialic acid residues present at

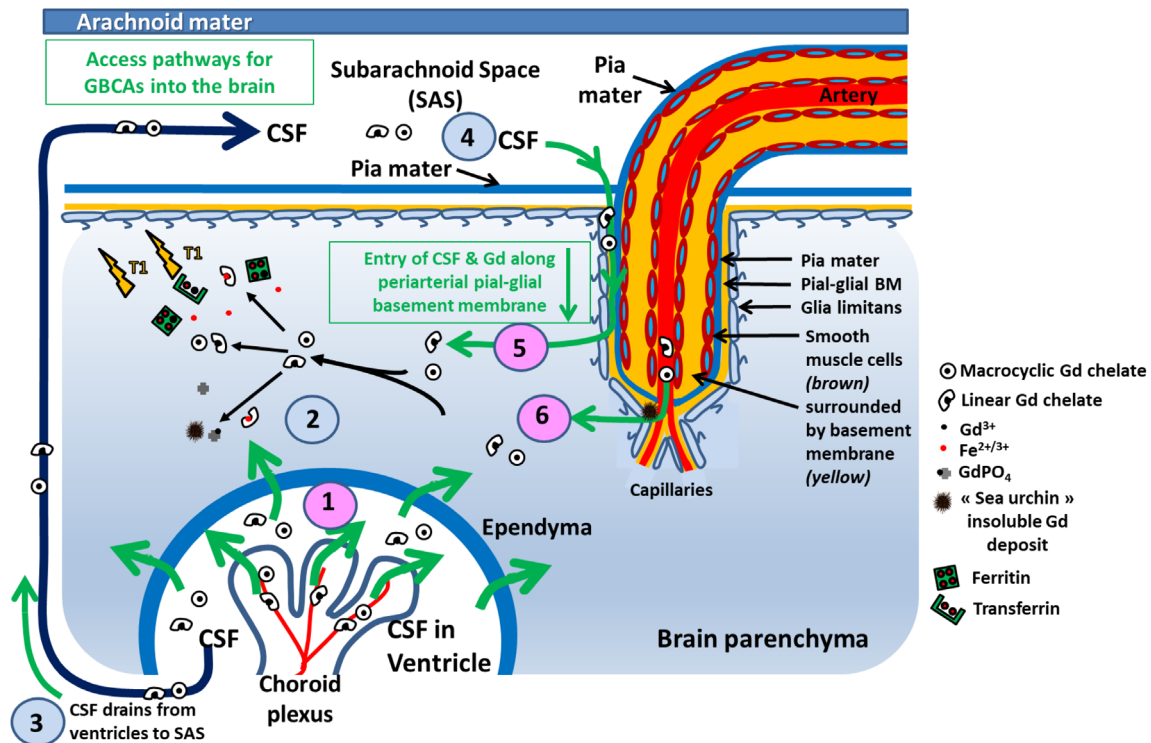


**FIGURE 4:** Summary of proposed inflow pathways for GBCAs in the brain. There appear to be three major pathways for the access of Gd into the brain (1) (pink) via the CSF and (6) (pink) directly from the blood. (1) GBCA enters the ventricular CSF from the blood via the blood-CSF barrier in the CP epithelium. (2) GBCA then enters the brain through the ependyma. (3) CSF containing GBCA flows from the ventricles into the subarachnoid space. (4) GBCA then enters the surface of the brain with CSF along periarterial pial-gliar basement membranes and (5) enters the brain parenchyma. (6) The third route for entry of GBCA into the brain is from the blood via the BBB in cerebral capillaries. The Gd speciation processes are summarized. Intact GBCAs (regardless of their chemical structure) cross the fenestrated capillaries of CP to access the CSF. Subsequently, the neutral molecules cross the ependymal lining to access the brain interstitium. Once present in the interstitium, low-stability (linear) GBCAs transmetallate with endogenous metals and dissociated Gd either precipitates in the form of spiny deposits and/or binds endogenous macromolecules, thus remaining trapped in the parenchyma. The GBCAs that remain in the CSF drain to cervical lymph nodes. CSF: cerebrospinal fluid; SAS: subarachnoid space.

the luminal pole of ependymal cells.<sup>78</sup> Therefore, this BSCFB pathway may be valid for neutral GBCAs only. Furthermore, the strongly anionic nature of the extracellular matrix (which contains large amounts of hyaluronan)<sup>79</sup> would probably impair the diffusion of negatively charged molecules such as ionic GBCAs.

After neutral GBCAs have diffused into the interstitium, they may reach metal-rich structures. This is especially the case with the dentate nucleus close to the 4<sup>th</sup> ventricle, or the globus pallidus.<sup>32–34</sup> In the case of rat DCN, we found that concentrations of endogenous elemental metals (ICP-MS) were in descending order: Fe ( $700 \pm 200$  nmol/g) > Zn ( $220 \pm 30$  nmol/g) > Cu ( $80 \pm 15$  nmol/g) (unpublished data). Subsequent to local transmetallation with endogenous metal, Gd dissociated from a linear GBCA would therefore be associated with Tf (76 kDa) or ferritin (450 kDa). Involvement of other macromolecules involved in the homeostasis of CNS metals may be also speculatively considered (calmodulin, parvalbumin, hyaluronic acid, etc.). Next, the Gd-macromolecules would be endocytosed into glial cells (and possibly neurons) and eventually accumulate in lysosomes in

the form of the nondegradable pigment lipofuscin,<sup>80,81</sup> as sometimes found associated with Gd deposits.<sup>42</sup> Anatomical proximity of CNS structures to the ventricles would indeed play a role in Gd uptake. Actually, both the endogenous metal concentration and anatomy should be considered together (for example, the thalamus is closer to the 3<sup>rd</sup> ventricle than the globus pallidus, but its Fe concentration is approximately four times lower).<sup>30</sup> The granular layer of the cerebellar cortex is rich in phosphorus,<sup>35</sup> a finding that may explain the absence of T<sub>1</sub> hypersignal at this level because of precipitation of Gd in the form of GdPO<sub>4</sub>.

#### Access Pathways Across the BBB

It has been stated that the presence of electron-dense Gd deposits within the interstitium would challenge the classical understanding of the impermeability of the BBB to GBCAs.<sup>60</sup> In rats, Gd deposits were found mainly in basement membranes or within cells around capillaries.<sup>42</sup>

It was initially reported that the electron-dense Gd deposits were located within endothelial cells.<sup>11,21</sup> Subsequently, a more detailed analysis revealed that they are located



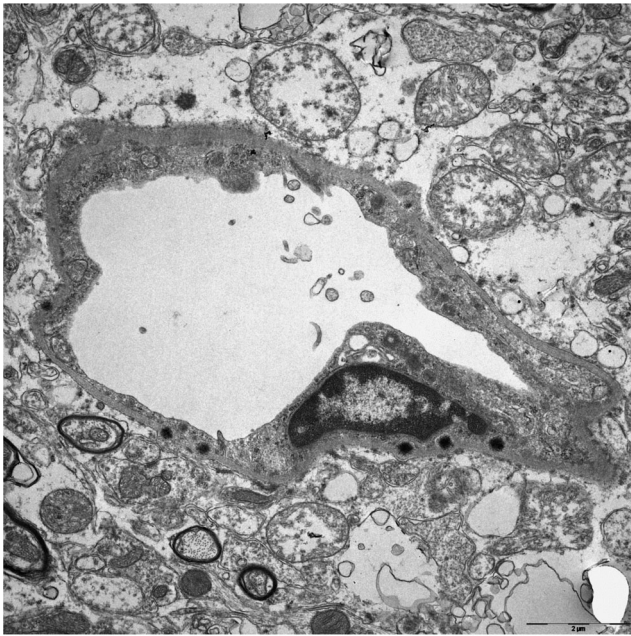


**FIGURE 5:** Typical aspect of sea-urchin Gd deposits localized in the basement membrane of a capillary. The presence of Gd was validated by electron energy loss spectroscopy (not shown).

in capillary basement membranes<sup>42</sup> (Figs. 5 and 6). This suggests that the Gd retained in the brain is also likely to be derived from the blood. Perivascular, Gd-containing deposits were also reported in the olfactory bulb of rats treated with linear GBCAs (gadodiamide and gadopentetate) but not the macrocyclic agent gadoterate.<sup>58</sup>

Colocation of Gd with P in the vicinity of vessels<sup>35,42</sup> is consistent with the precipitation of Gd in the form of  $\text{GdPO}_4$  present in the sea urchin-shaped deposits found.<sup>82</sup> This phenomenon might result from transmetallation with calcium, a metal crucial for the tight regulation of cerebral blood flow at the level of the neurovascular unit.<sup>83</sup>

However, the presence of insoluble Gd deposits should not preclude the possibility of soluble Gd species (undetectable by TEM).

#### THE PERIVASCULAR (PIAL-GLIAL) ACCESS PATHWAY.

The involvement of the “glymphatic” system<sup>84</sup> in the distribution and clearance of GBCAs from brain parenchyma is currently the subject of much speculation.<sup>68,85–89</sup>

Actually, the “glymphatic” concept needs to be refined, especially with regard to the role of glia and transfer of solutes into the extracellular spaces (ECS) of the brain.<sup>89</sup> There are arguments against the involvement of the “glymphatic” system, at least as it was initially proposed. First, it would involve aquaporin 4 (AQP4) localized to astrocyte endfeet and anchored to the perivascular basement membrane.<sup>90</sup> It is unclear whether AQP4 is involved in the passage of GBCAs. Actually, the pore in each monomer of AQP4 narrows to  $\sim 2.8 \text{ \AA}$ ,<sup>90</sup> thus effectively excluding the permeation of

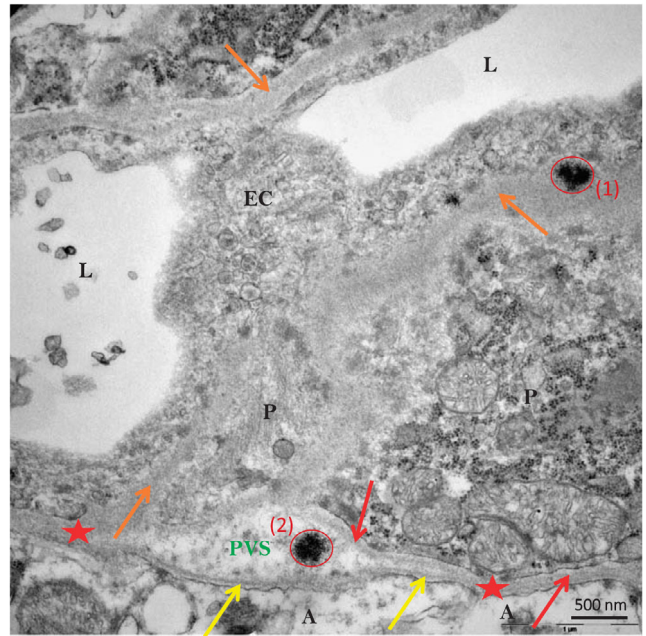


**FIGURE 6:** Sea urchin-like, spheroid-shaped Gd deposits (red circles) localized in the basement membrane (1) and in the perivascular space (2) of a capillary (from the DCN of a gadodiamide-treated rat). A indicates astrocyte end-feet; yellow arrows indicate basement membranes of glia limitans; orange arrows indicate unified basement membranes of endothelial cell and pericyte abluminal side; red arrows indicate basement membrane of one pericyte abluminal side; red stars indicate basement membrane coalescence of glia limitans and pericyte or of endothelial cell; EC, endothelial cell; L, vessel lumen; P, pericyte. The presence of Gd was validated by electron energy loss spectroscopy (not shown). Reprinted from Ref. 42, modified, with permission.

molecules larger than water. Studies in  $Aqp4^{-/-}$  mice may allow this issue to be elucidated. Furthermore, it was initially suggested (in studies using an ionic GBCA as tracer) that the outflow pathway from the brain parenchyma was alongside veins.<sup>91</sup> However, subsequent experiments have shown that when tracers in the CSF enter the brain, they do so along pial-glial basement membranes and then they flow out of the brain along intramural peri-arterial drainage (IPAD) pathways within 30 minutes and not along the walls of veins.<sup>92,93</sup> Finally, the hydraulic resistance of the brain ECS would restrict the convective flow, as initially proposed.<sup>89</sup>

The existence of PVS around arteries as they penetrate the cerebral cortex is disputed<sup>94</sup> and may actually be related to the presence of artifactual swelling of astrocytes.<sup>95</sup>

We propose that water-soluble substances in the CSF enter the surface of the brain along periarial pial-glial basement membranes (Fig. 4) and leave the brain along IPAD pathways, one of the major routes for the drainage of brain fluid and solutes and a very rapid process.<sup>93,96</sup>

In addition to the BCSFB pathway, it is therefore proposed that GBCAs enter the brain parenchyma through the perivascular pial-glial basement membranes system (Fig. 4),

consistent with LA-ICP-MS data<sup>35</sup> and recent advances in the field.<sup>96</sup>

Lastly, an MRI study suggested that GBCA enters the aqueous chamber of the eye following infiltration via the ciliary body and drainage along the perineural space of the optic nerve.<sup>68</sup> Following intrathecal administration of a GBCA, an increase in T<sub>1</sub> SI was observed within the optic nerve, optic chiasm, optic tract, and primary visual cortex, thus indicating direct communication between CSF of the subarachnoid space and the extravascular space of the visual pathway. The drainage of fluid and solutes from the eye is only now being clarified.<sup>97</sup> Interestingly, one case report has shown insoluble Gd deposits in and around blood vessels of the choriocapillaris of the eye.<sup>98</sup>

### CLEARANCE PATHWAYS

It is likely that, in the event that GBCAs present in the interstitial fluid (ISF) of the brain do not cross metal-rich structures or are unable to transmetallate with an endogenous metal, they will drain out of the interstitium along basement membranes in the walls of capillaries as well as along basement membranes in the tunica media of cerebral arterioles and arteries (the IPAD pathway) (Fig. 7).<sup>99</sup> The physiological IPAD pathway is situated within the smooth muscle cell basement membranes in the tunica media of the arteries.<sup>96</sup> This

drainage phenomenon is very rapid, which may explain why it has not been shown so far in the case of GBCAs. However, long-term washout of intact GBCAs may follow another, still unknown, pathway. Importantly, the entry and outflow pathways are anatomically distinct.<sup>93</sup>

Lastly, most of the evidence suggests that only ~15% of tracers draining along the IPAD pathway pass into the CSF, whereas the remaining ~85% of the tracer travels along the walls of intracranial arteries to cervical lymph nodes.<sup>100</sup>

### LYMPHATIC DRAINAGE

There are no lymphatic vessels in the brain parenchyma, but there is lymphatic drainage of interstitial fluid from the brain to lymph nodes of the neck along the walls of cerebral arteries.<sup>101</sup> This drainage is via the IPAD pathways along basement membranes of capillaries and between smooth muscle cells in the walls of arteries.<sup>92-94,99</sup>

### CONCLUSION

The finding of T<sub>1</sub> hypersignal in the brain of patients who repeatedly received linear GBCAs led to a very large number of nonclinical and clinical studies that profoundly challenged several dogma regarding the distribution of GBCAs in the healthy brain. It seems important to distinguish between “physiological” distribution and excretion of chelated GBCAs

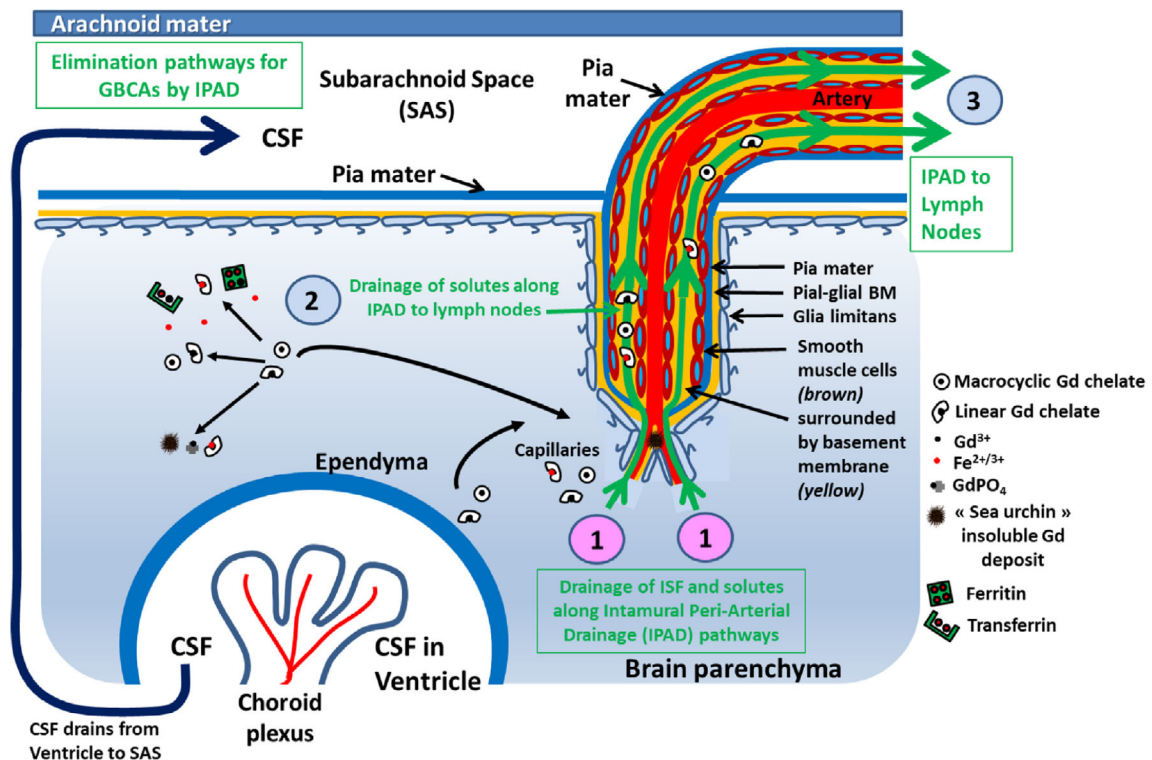


FIGURE 7: The clearance pathway (Intramural Peri-Arterial Drainage, IPAD). (1) IPAD begins with the entry of interstitial fluid ISF and solutes from the brain parenchyma into basement membranes in the walls of cerebral capillaries. (2) Fluid and solutes then drain into the IPAD pathways in the basement membranes that surround smooth muscle cells in the tunica media of arteries. (3) It is along the IPAD pathway that fluid and solutes are eliminated from the brain through drainage to lymph nodes.

from the brain parenchyma from Gd deposition that follows repeated administrations of linear GBCAs and which is driven by their thermodynamic properties. The follow up, by MRI, of the still chelated, intact, GBCAs may have useful clinical implications.<sup>68</sup> In this review, we propose three access pathways for GBCAs into the brain parenchyma:

1. Entry into the CSF via the choroid plexus and then from the CSF through the walls of the ventricles directly into the brain;
2. From the CSF in the subarachnoid space along penetrating arteries in periarterial (periarteriolar) pial-glia basement membranes;
3. From blood through the BBB (Gd found in the basement membranes of capillaries).

The outflow pathway for Gd in the interstitial fluid of the brain parenchyma is most probably along basement membranes in the walls of cerebral capillaries and arteries as the IPAD pathways.<sup>92–94,99</sup>

### Grant Support

No grant support.

## ACKNOWLEDGMENTS

The authors thank Claire Corot, PharmD, PhD, Philippe Robert, PhD, and Aymeric Seron, PhD, for helpful discussions.

## REFERENCES

1. Lohrke J, Frenzel T, Endrikat J, et al. 25 years of contrast-enhanced MRI: Developments, current challenges and future perspectives. *Adv Ther* 2016;33:1-28.
2. Essig M, Dinkel J, Gutierrez JE. Use of contrast media in neuroimaging. *Magn Reson Imaging Clin N Am* 2012;20:633-648.
3. Zhang Y, Cao Y, Shih GL, Hecht EM, Prince MR. Extent of signal hyperintensity on unenhanced T1-weighted brain MR images after more than 35 administrations of linear gadolinium-based contrast agents. *Radiology* 2017;282:516-525.
4. Khant ZA, Hirai T, Kadota Y, et al. T1 shortening in the cerebral cortex after multiple administrations of gadolinium-based contrast agents. *Magn Reson Med* 2017;16:84-86.
5. Kanda T, Ishii K, Kawaguchi H, Kitajima K, Takenaka D. High signal intensity in the dentate nucleus and globus pallidus on unenhanced T1-weighted MR images: Relationship with increasing cumulative dose of a gadolinium-based contrast material. *Radiology* 2014;270:834-841.
6. Mallio CA, Lo Vullo G, Messina L, Beomonte Zobel B, Parizel PM, Quattrocchi CC. Increased T1 signal intensity of the anterior pituitary gland on unenhanced magnetic resonance images after chronic exposure to gadodiamide. *Invest Radiol* 2020;55:25-29.
7. Chehabeddine L, Al Saleh T, Baalbaki M, Saleh E, Khoury SJ, Hannoun S. Cumulative administrations of gadolinium-based contrast agents: Risks of accumulation and toxicity of linear vs macrocyclic agents. *Crit Rev Toxicol* 2019;49:262-279.
8. Roberts DR, Holden KR. Progressive increase of T1 signal intensity in the dentate nucleus and globus pallidus on unenhanced T1-weighted MR images in the pediatric brain exposed to multiple doses of gadolinium contrast. *Brain Dev* 2016;38:331-336.

### Rasschaert et al.: GBCAs Distribution in Brain Parenchyma

9. Roberts DR, Welsh CA, LeBel DP 2nd, Davis WC. Distribution map of gadolinium deposition within the cerebellum following GBCA administration. *Neurology* 2017;88:1206-1208.
10. Robert P, Violas X, Grand S, et al. Linear gadolinium-based contrast agents are associated with brain gadolinium retention in healthy rats. *Invest Radiol* 2016;51:73-82.
11. Lohrke J, Frisk AL, Frenzel T, et al. Histology and gadolinium distribution in the rodent brain after the administration of cumulative high doses of linear and macrocyclic gadolinium-based contrast agents. *Invest Radiol* 2017;52:324-333.
12. Fretellier N, Granottier A, Rasschaert M, et al. Does age interfere with gadolinium toxicity and presence in brain and bone tissues? A comparative gadoterate versus gadodiamide study in juvenile and adult rats. *Invest Radiol* 2019;54:61-71.
13. Boyken J, Frenzel T, Lohrke J, Jost G, Pietsch H. Gadolinium accumulation in the deep cerebellar nuclei and globus pallidus after exposure to linear but not macrocyclic gadolinium-based contrast agents in a retrospective pig study with high similarity to clinical conditions. *Invest Radiol* 2018;53:278-285.
14. Radbruch A, Richter H, Fingerhut S, et al. Gadolinium deposition in the brain in a large animal model: Comparison of linear and macrocyclic gadolinium-based contrast agents. *Invest Radiol* 2019;54:531-536.
15. Robic C, Port M, Rousseaux O, et al. Physicochemical and pharmacokinetic profiles of gadopipiclenol: A new macrocyclic gadolinium chelate with high T1 relaxivity. *Invest Radiol* 2019;54:475-484.
16. Radbruch A. Are some agents less likely to deposit gadolinium in the brain? *Magn Reson Imaging* 2016;34:1351-1354.
17. Smith TE, Steven A, Bagert BA. Gadolinium deposition in neurology clinical practice. *Ochsner J* 2019;19:17-25.
18. Thomsen HS, Morcos SK, Almén T, et al. Nephrogenic systemic fibrosis and gadolinium-based contrast media: Updated ESUR contrast medium safety committee guidelines. *Eur Radiol* 2013;23:307-318.
19. European Medicines Agency. EMA's final opinion confirms restrictions on use of linear gadolinium agents in body scans. November 11, 2017. [http://www.ema.europa.eu/docs/en\\_GB/document\\_library/Referrals\\_document/gadolinium\\_contrast\\_agents\\_31/European\\_Commission\\_final\\_decision/WC500240575.pdf](http://www.ema.europa.eu/docs/en_GB/document_library/Referrals_document/gadolinium_contrast_agents_31/European_Commission_final_decision/WC500240575.pdf).
20. Food and Drug Administration. Drug Safety Communication: FDA warns that gadolinium-based contrast agents (GBCAs) are retained in the body; requires new class warnings. December 19, 2017. <https://www.fda.gov/media/109825/download>
21. McDonald RJ, McDonald JS, Kallmes DF, et al. Intracranial gadolinium deposition after contrast-enhanced MR imaging. *Radiology* 2015;275:772-782.
22. Kanda T, Fukusato T, Matsuda M, et al. Gadolinium-based contrast agent accumulates in the brain even in subjects without severe renal dysfunction: Evaluation of autopsy brain specimens with inductively coupled plasma mass spectroscopy. *Radiology* 2015;276:228-232.
23. Kartamihardja AA, Nakajima T, Kameo S, Koyama H, Tsushima Y. Distribution and clearance of retained gadolinium in the brain: Differences between linear and macrocyclic gadolinium based contrast agents in a mouse model. *Br J Radiol* 2016;89:20160509.
24. Robert P, Fingerhut S, Factor C, et al. One-year retention of gadolinium in the brain: Comparison of gadodiamide and gadoterate meglumine in a rodent model. *Radiology* 2018;288:424-433.
25. Gianolio E, Bardini P, Arena F, et al. Gadolinium retention in the rat brain: Assessment of the amounts of insoluble gadolinium-containing species and intact gadolinium complexes after repeated administration of gadolinium-based contrast agents. *Radiology* 2017;285:839-849.
26. Rasschaert M, Idée JM, Robert P, et al. Moderate renal failure accentuates T1 signal enhancement in the deep cerebellar nuclei of gadodiamide-treated rats. *Invest Radiol* 2017;52:255-264.
27. Rasschaert M, Emerit A, Fretellier N, et al. Gadolinium retention, brain T1 hyperintensity, and endogenous metals: A comparative study of

- macrocyclic versus linear gadolinium chelates in renally sensitized rats. *Invest Radiol* 2018;53:328-337.
28. Errante Y, Cirimele V, Mallio CA, Di Lazzaro V, Zobel BB, Quattrocchi CC. Progressive increase of T1 signal intensity of the dentate nucleus on unenhanced magnetic resonance images is associated with cumulative doses of intravenously administered gadodiamide in patients with normal renal function, suggesting dechelation. *Invest Radiol* 2014;49:685-690.
  29. Port M, Idée JM, Medina C, Robic C, Sabatou M, Corot C. Efficiency, thermodynamic and kinetic stability of marketed gadolinium chelates and their possible clinical consequences: A critical review. *Biometals* 2008;21:469-490.
  30. Hallgren B, Sourander P. The effect of age on the non-haemin iron in the human brain. *J Neurochem* 1958;3:41-51.
  31. Hasan KM, Walimuni IS, Kramer LA, Narayana PA. Human brain iron mapping using atlas-based T2 relaxometry. *Magn Reson Med* 2012;67:731-739.
  32. Popescu BF, Robinson CA, Rajput A, Rajput AH, Harder SL, Nichol H. Iron, copper, and zinc distribution of the cerebellum. *Cerebellum* 2009;8:74-79.
  33. Popescu BF, Nichol H. Mapping brain metals to evaluate therapies for neurodegenerative disease. *CNS Neurosci Ther* 2011;17:256-268.
  34. Koeppen AH, Ramirez RL, Yu D, et al. Friedreich's ataxia causes redistribution of iron, copper, and zinc in the dentate nucleus. *Cerebellum* 2012;11:845-860.
  35. Fingerhut S, Sperling M, Holling M, et al. Gadolinium-based contrast agents induce gadolinium deposits in cerebral vessel walls, while the neuropil is not affected: An autopsy study. *Acta Neuropathol* 2018;136:127-138.
  36. Ward RJ, Zucca FA, Duyn JH, Crichton RR, Zecca L. The role of iron in brain ageing and neurodegenerative disorders. *Lancet Neurol* 2014;13:1045-1060.
  37. Cabantchik ZI. Labile iron in cells and body fluids: Physiology, pathology, and pharmacology. *Front Pharmacol* 2014;5:45.
  38. Zak O, Aisen P. Spectroscopic and thermodynamic studies on the binding of gadolinium(III) to human serum transferrin. *Biochemistry* 1988;27:1075-1080.
  39. Motekaitis RJ, Sun Y, Martell AE. New synthetic, selective, high-affinity ligands for effective trivalent metal ion binding and transport. *Inorg Chim Acta* 1992;198-200:421-428.
  40. Abraham JL, Thakral C, Skov L, Rossen K, Marckmann P. Dermal inorganic gadolinium concentrations: Evidence for in vivo transmetallation and long-term persistence in nephrogenic systemic fibrosis. *Br J Dermatol* 2008;158:273-280.
  41. Idée JM, Berthommier C, Goulas V, et al. Haemodynamic effects of macrocyclic and linear gadolinium chelates in rats: Role of calcium and transmetallation. *Biometals* 1998;11:113-123.
  42. Rasschaert M, Schroeder JA, Wu TD, et al. Multimodal imaging study of gadolinium presence in rat cerebellum: Differences between Gd chelates, presence in the Virchow-Robin space, association with lipofuscin, and hypotheses about distribution pathway. *Invest Radiol* 2018;53:518-528.
  43. Fingerhut S, Niehoff AC, Sperling M, et al. Spatially resolved quantification of gadolinium deposited in the brain of a patient treated with gadolinium-based contrast agents. *J Trace Elem Med Biol* 2018;45:125-130.
  44. Clases D, Fingerhut S, Jeibmann A, Sperling M, Doble P, Karst U. LA-ICP-MS/MS improves limits of detection in elemental bioimaging of gadolinium deposition originating from MRI contrast agents in skin and brain tissues. *J Trace Elem Med Biol* 2019;51:212-218.
  45. El-Khatib AH, Radbruch H, Trog S, et al. Gadolinium in human brain sections and colocalization with other elements. *Neurol Neuroimmunol Neuroinflamm* 2018;6:e515.
  46. Frenzel T, Apte C, Jost G, Schöckel L, Lohrke J, Pietsch H. Quantification and assessment of the chemical form of residual gadolinium in the brain after repeated administration of gadolinium-based contrast agents: Comparative study in rats. *Invest Radiol* 2017;52:396-404.
  47. Boyken J, Frenzel T, Lohrke J, Jost G, Schütz G, Pietsch H. Impact of treatment with chelating agents depends on the stability of administered GBCAs: A comparative study in rats. *Invest Radiol* 2019;54:76-82.
  48. Kartamihardja AAP, Hanaoka H, Andriana P, et al. Quantitative analysis of Gd in the protein content of the brain following single injection of gadolinium-based contrast agents (GBCAs) by size exclusion chromatography. *Br J Radiol* 2019;92:20190062.
  49. Strzeminska I, Factor C, Robert P, et al. Long-term evaluation of gadolinium retention in rat brain after single injection of a clinically relevant dose of gadolinium-based contrast agents. *Invest Radiol* 2020;55:138-143.
  50. Taupitz M, Stolzenburg N, Ebert M, et al. Gadolinium-containing magnetic resonance contrast media: Investigation on the possible transchelation of Gd<sup>3+</sup> to the glycosaminoglycan heparin. *Contrast Media Mol Imaging* 2013;8:108-116.
  51. Idée JM, Port M, Dencausse A, Lancelot E, Corot C. Involvement of gadolinium chelates in the mechanism of nephrogenic systemic fibrosis: An update. *Radiol Clin North Am* 2009;47:855-869.
  52. Jost G, Frenzel T, Boyken J, Lohrke J, Nischwitz V, Pietsch H. Long-term excretion of gadolinium-based contrast agents: Linear versus macrocyclic agents in an experimental rat model. *Radiology* 2019;290:340-348.
  53. Cao Y, Zhang Y, Shih G, et al. Effect of renal function on gadolinium-related signal increases on unenhanced T1-weighted brain magnetic resonance imaging. *Invest Radiol* 2016;51:677-682.
  54. Jost G, Frenzel T, Lohrke J, Lenhard DC, Naganawa S, Pietsch H. Penetration and distribution of gadolinium-based contrast agents into the cerebrospinal fluid in healthy rats: A potential pathway of entry into the brain tissue. *Eur Radiol* 2017;27:2877-2885.
  55. Nehra AK, McDonald RJ, Bluhm AM, et al. Accumulation of gadolinium in human cerebrospinal fluid after gadobutrol-enhanced MR imaging: A prospective observational cohort study. *Radiology* 2018;288:416-423.
  56. Berger F, Kubik-Huch RA, Niemann T, et al. Gadolinium distribution in cerebrospinal fluid after administration of a gadolinium-based MR contrast agent in humans. *Radiology* 2018;288:703-709.
  57. Kartamihardja AA, Nakajima T, Kameo S, Koyama H, Tsumishima Y. Impact of impaired renal function on gadolinium retention after administration of gadolinium-based contrast agents in a mouse model. *Invest Radiol* 2016;51:655-660.
  58. Wang ST, Hua ZX, Fan DX, Zhang X, Ren K. Gadolinium retention and clearance in the diabetic brain after administrations of gadodiamide, gadopentetate dimeglumine, and gadoterate meglumine in a rat model. *Biomed Res Int* 2019;2019:3901907.
  59. McGann JP. Poor human olfaction is a 19th-century myth. *Science* 2017;356:eeeam7263.
  60. McDonald RJ, McDonald JS, Dai D, et al. Comparison of gadolinium concentrations within multiple rat organs after intravenous administration of linear versus macrocyclic gadolinium chelates. *Radiology* 2017;285:536-545.
  61. McDonald RJ, McDonald JS, Kallmes DF, et al. Gadolinium deposition in human brain tissues after contrast-enhanced MR imaging in adult patients without intracranial abnormalities. *Radiology* 2017;285:546-554.
  62. Paxinos G, Watson C. *The rat brain in stereotaxic coordinates*. 6th ed. London: Elsevier Academic Press; 2007. p 461.
  63. Pesch B, Dydak U, Lotz A, et al. Association of exposure to manganese and iron with relaxation rates R1 and R2\*—Magnetic resonance imaging results from the WELDOX II study. *Neurotoxicology* 2018;64:68-77.
  64. Mamourian AC, Hoopes PJ, Lewis LD. Visualization of intravenously administered contrast material in the CSF on fluid-attenuated

- inversion-recovery MR images: An in vitro and animal-model investigation. *AJNR Am J Neuroradiol* 2000;21:105-111.
65. Bozzao A, Floris R, Fasoli F, Fantozzi LM, Colonnese C, Simonetti G. Cerebrospinal fluid changes after intravenous injection of gadolinium chelate: Assessment by FLAIR MR imaging. *Eur Radiol* 2003;13:592-597.
  66. Morris JM, Miller GM. Increased signal in the subarachnoid space on fluid-attenuated inversion recovery imaging associated with the clearance dynamics of gadolinium chelate: A potential diagnostic pitfall. *AJNR Am J Neuroradiol* 2007;28:1964-1967.
  67. Naganawa S, Suzuki K, Yamazaki M, Sakurai Y, Ikeda M. Time course for measuring endolymphatic size in healthy volunteers following intravenous administration of gadoteridol. *Magn Reson Med Sci* 2014;13:73-80.
  68. Deike-Hofmann K, Reuter J, Haase R, et al. Glymphatic pathway of gadolinium-based contrast agents through the brain: Overlooked and misinterpreted. *Invest Radiol* 2019;54:229-237.
  69. Strazielle N, Ghersi-Egea JF. Choroid plexus in the central nervous system: Biology and physiopathology. *J Neuropathol Exp Neurol* 2000;59:561-574.
  70. Praetorius J, Damkier HH. Transport across the choroid plexus epithelium. *Am J Physiol Cell Physiol* 2017;312:C673-C686.
  71. Liddelow SA. Development of the choroid plexus and blood-CSF barrier. *Front Neurosci* 2015;9:32.
  72. Khasawneh AH, Garling RJ, Harris CA. Cerebrospinal fluid circulation: What do we know and how do we know it? *Brain Circ* 2018;4:14-18.
  73. De Leon MJ, Li Y, Okamura N, et al. Cerebrospinal fluid clearance in Alzheimer disease measured with dynamic PET. *J Nucl Med* 2017;58:1471-1476.
  74. Louveau A, Smirnov I, Keyes TJ, et al. Structural and functional features of central nervous system lymphatic vessels. *Nature* 2015;523:337-341.
  75. Kida S, Pantazis A, Weller RO. CSF drains directly from the subarachnoid space into nasal lymphatics in the rat. *Anatomy, histology and immunological significance. Neuropathol Appl Neurobiol* 1993;19:480-488.
  76. Roales-Buján R, Páez P, Guerra M, et al. Astrocytes acquire morphological and functional characteristics of ependymal cells following disruption of ependyma in hydrocephalus. *Acta Neuropathol* 2012;124:531-546.
  77. Bui JD, Nammari DR, Buckley DL, et al. In vivo dynamics and distribution of intracerebroventricularly administered gadodiamide, visualized by magnetic resonance imaging. *Neuroscience* 1999;90:1115-1122.
  78. Wan XM, Fu TC, Smith PH, Brainard JR, London RE. Magnetic resonance imaging study of the rat cerebral ventricular system utilizing intracerebrally administered contrast agents. *Magn Reson Med* 1991;21:97-106.
  79. Oohashi T, Edamatsu M, Bekku Y, Carulli D. The hyaluronan and proteoglycan link proteins: Organizers of the brain extracellular matrix and key molecules for neuronal function and plasticity. *Exp Neurol* 2015;274:134-144.
  80. Sulzer D, Mosharov E, Tallozy Z, Zucca FA, Simon JD, Zecca L. Neuronal pigmented autophagic vacuoles: Lipofuscin, neuromelanin, and ceroid as macroautophagic responses during aging and disease. *J Neurochem* 2008;106:24-36.
  81. Kurz T, Terman A, Gustafsson B, Brunk UT. Lysosomes in iron metabolism, ageing and apoptosis. *Histochem Cell Biol* 2008;129:389-406.
  82. Li R, Ji Z, Chang CH, et al. Surface interactions with compartmentalized cellular phosphates explain rare earth oxide nanoparticle hazard and provide opportunities for safer design. *ACS Nano* 2014;8:1771-1783.
  83. McConnell HL, Kersch CN, Woltjer RL, Neuwelt EA. The translational significance of the neurovascular unit. *J Biol Chem* 2017;292:762-770.
  84. Jessen NA, Munk AS, Lundgaard I, Nedergaard M. The glymphatic system: A beginner's guide. *Neurochem Res* 2015;40:2583-2599.
  85. Eide PK, Ringstad G. MRI with intrathecal MRI gadolinium contrast medium administration: A possible method to assess glymphatic function in human brain. *Acta Radiol Open* 2015;4:2058460115609635.
  86. Lee H, Mortensen K, Sanggaard S, et al. Quantitative Gd-DOTA uptake from cerebrospinal fluid into rat brain using 3D VFA-SPGR at 9.4T. *Magn Reson Med* 2018;79:1568-1578.
  87. Taoka T, Jost G, Frenzel T, Naganawa S, Pietsch H. Impact of the glymphatic system on the kinetic and distribution of gadodiamide in the rat brain: Observations by dynamic MRI and effect of circadian rhythm on tissue gadolinium concentrations. *Invest Radiol* 2018;53:529-534.
  88. Taoka T, Naganawa S. Glymphatic imaging using MRI. *J Magn Reson Imaging* 2020;51:11-24.
  89. Abbott NJ, Pizzo ME, Preston JE, Janigro D, Thorne RG. The role of brain barriers in fluid movement in the CNS: Is there a 'glymphatic' system? *Acta Neuropathol* 2018;135:387-407.
  90. Nagelhus EA, Ottersen OP. Physiological roles of aquaporin-4 in brain. *Physiol Rev* 2013;93:1543-1562.
  91. Iliff JJ, Lee H, Yu M, et al. Brain-wide pathway for waste clearance captured by contrast-enhanced MRI. *J Clin Invest* 2013;123:1299-1309.
  92. Arbel-Ornath M, Hudry E, Eikermann-Haerter K, et al. Interstitial fluid drainage is impaired in ischemic stroke and Alzheimer's disease mouse models. *Acta Neuropathol* 2013;126:353-364.
  93. Albargothy NJ, Johnston DA, MacGregor-Sharp M, et al. Convective influx/glymphatic system: Tracers injected into the CSF enter and leave the brain along separate periarterial basement membrane pathways. *Acta Neuropathol* 2018;136:139-152.
  94. Weller RO, Sharp MM, Christodoulides M, Carare RO, Møllgård K. The meninges as barriers and facilitators for the movement of fluid, cells and pathogens related to the rodent and human CNS. *Acta Neuropathol* 2018;135:363-385.
  95. Sapsford I, Buontempo J, Weller RO. Basement membrane surface and perivascular compartments in normal human brain and glial tumours. A scanning electron microscope study. *Neuropathol Appl Neurobiol* 1983;9:181-194.
  96. Morris AW, Sharp MM, Albargothy NJ, et al. Vascular basement membranes as pathways for the passage of fluid into and out of the brain. *Acta Neuropathol* 2016;131:725-736.
  97. Jacobsen HH, Ringstad G, Jørstad ØK, Moe MC, Sandell T, Eide PK. The human visual pathway communicates directly with the subarachnoid space. *Invest Ophthalmol Vis Sci* 2019;60:2773-2780.
  98. Barker-Griffith A, Goldberg J, Abraham JL. Ocular pathologic features and gadolinium deposition in nephrogenic systemic fibrosis. *Arch Ophthalmol* 2011;129:661-663.
  99. Carare RO, Bernardes-Silva M, Newman TA, et al. Solutes, but not cells, drain from the brain parenchyma along basement membranes of capillaries and arteries: Significance for cerebral amyloid angiopathy and neuroimmunology. *Neuropathol Appl Neurobiol* 2008;34:131-144.
  100. Szentistvanyi I, Patlak CS, Ellis RA, Cserr HF. Drainage of interstitial fluid from different regions of rat brain. *Am J Physiol* 1984;246:F835-F844.
  101. Yamada S, DePasquale M, Patlak CS, Cserr HF. Albumin outflow into deep cervical lymph from different regions of rabbit brain. *Am J Physiol* 1991;261:H1197-H1204.